scientific reports

Check for updates

OPEN

Ultrasonic layer resonance assisted adhesive bonding for metal plates

Toru Hakkaku, Naoki Mori✉ & Takahiro Hayashi

Adhesive bonding can be enhanced with appropriate pretreatment methods, one of which includes the application of mechanical vibrations to uncured adhesives on a substrate. Previous studies have shown that high-power ultrasonic vibrations at low frequencies promote wettability between the adhesive and substrate, resulting in increased bond strength after the cure. High-frequency ultrasounds may also affect adhesion due to their unique phenomenon resulting from shorter wavelengths, but that remains unexplored. In this paper, an ultrasonic treatment assisted by layer resonance is proposed for adhesive joints. Ultrasonic vibrations are applied to a curing adhesive layer based on the resonance frequencies measured by the ultrasonic pulse-echo technique. Tensile shear tests demonstrate that the resonance of a curing adhesive layer can enhance bond strength after the cure. In particular, this treatment is shown to be effective if a frequency sweep is adopted according to an increase in the resonance frequency due to the curing process. The improvement in bond strength is associated with the relation between the processing time in the proposed treatment and the pot life of the adhesive, depending on the type of adhesive used. The findings of this paper show that the proposed treatment can improve bond strength but requires appropriate processing conditions depending on the bonding situations.

Keywords Adhesive bonding, Pretreatment, Ultrasound, Layer resonance, Curing monitoring

Adhesive bonding is expanding its applications in different industrial fields due to the progress of adhesive materials and surface preparation technologies. Mechanical fastening is an essential joining technique to manufacture various structures and products, but it requires fasteners that increase weight. Replacing such mechanical fasteners with adhesive bonds leads to weight reduction, which would bring multiple benefits, e.g., the improvement in energy efficiency.

However, a technical challenge remains in the adhesive bonding technology to promote its applications further, namely, suppression of bonding quality variation. Mechanical and chemical interactions between substrate and adhesive are essential to create bonding, which is highly sensitive to bonding conditions such as adhesive curing conditions and adherend surface preparation. Different types of surface preparation have been extensively explored in previous studies to enhance and guarantee adhesion between substrate and adhesive, including sandblasting[1,2] anodic oxidation[3,4] and laser pretreatment[5–9].

In the last few decades, ultrasonic pretreatment has been drawing attention as an effective method to improve bong strength, which is called ultrasonic-assisted adhesive bonding[10–14]. High-power ultrasonic vibrations input into an uncured adhesive enhance its wettability and remove microbubbles inside the adhesive layer, increasing bond strength after curing under appropriate conditions. Holtmannspötter and co-workers[15] developed an adhesive supplier with a high-power ultrasonic transducer, which helps to support interface formation by eliminating contamination on adherend surfaces. Yang and co-workers[16,17] proposed an ultrasonic vibration-assisted preprocessing for adhesive bonding of carbon fiber reinforced plastic (CFRP) composite laminates using an ultrasonic cleaner, demonstrating that tensile shear strength and mode-I fracture toughness are improved. Wang and co-workers[18] attached an ultrasonic horn not on joint surfaces but on a substrate and demonstrated by capillary experiment that the ultrasonic vibration can increase pressure inside the adhesive. Ultrasonic-assisted treatment has been applied in the fields of not only adhesion in manufacturing but also bioadhesion between tissue and hydrogel[19]. These previous techniques usually employ high-power ultrasonic vibrations at low frequencies below tens of kilohertz to vibrate substrates and adhesives strongly.

On the other hand, to the authors' knowledge, the application of ultrasounds with frequencies higher than 1 MHz has not been explored in the preprocessing to assist adhesive bonding, although they are extensively used in nondestructive testing and characterization for adhesively bonded joints after curing. Exciting large displacements at high frequencies is difficult, but their vibrations are fast and can show spatial distributions within layers. This feature brings a unique phenomenon that cannot appear in low frequency ranges, namely, layer

Department of Mechanical Engineering, Graduate School of Engineering, The University of Osaka, Osaka, Japan. ✉email: n.mori@mech.eng.osaka-u.ac.jp

resonance[20–25]. For example, when a planar layer is exposed to the incidence of an ultrasonic wave propagating in the thickness direction, a standing wave can be generated within the layer, amplifying its vibration. Since the layer resonance frequencies can be related to the layer thickness and the ultrasonic wavelength, their measurements can lead to the characterization of the elastic property of adhesive layers after curing[26]. Moreover, recently, the authors have demonstrated that curing adhesive layers show resonance for ultrasonic incidence[27]. It has been shown that the layer resonance frequencies tend to increase as the curing proceeds because the elastic property of the adhesive increases. If the input of high-frequency ultrasounds into curing adhesives can promote the adhesion to substrates, simultaneously probing and reinforcing adhesion states might be possible. However, this attempt has not been reported yet.

The present paper aims to explore high-frequency ultrasonic-assisted treatment using layer resonance to improve adhesion between adhesive and metal substrate. Based on the measured resonance frequency of a curing adhesive layer, the effects of input vibration signals are investigated for single lap joints. After the cure, tensile shear tests are conducted to determine bond strength, and the fracture surfaces are observed to identify the fracture behavior.

In the next section, the procedures for resonance frequency measurement are first presented. The layer resonance frequencies are identified by measuring the ultrasonic reflection spectrum from the adhesive layer.

Experimental methods

Identification of layer resonance frequency by ultrasonic pulse-echo measurement

In this study, ultrasonic resonance treatment is proposed, and its effects on bonding strength and fracture configuration are examined for single-lap adhesively bonded joints. The proposed technique consists of two stages: measuring resonance frequency and applying ultrasonic vibrations. This section provides the theoretical background of layer resonance and presents the procedures for measuring the resonance frequencies of adhesive layers.

When a planar adhesive layer sandwiched by metal adherends is subjected to normal incidence of a longitudinal wave, layer resonance occurs at frequencies

$$f_n = \frac{nc}{2h}, \tag{1}$$

where $n = 1, 2, \ldots$ is the resonance order, c is the wave velocity of the adhesive, and h is the bond thickness[27]. The viscosity of the adhesive is usually not so significant that its effect is neglected in Eq. (1). At these frequencies, standing waves are formed within the adhesive layer, amplifying the vibration amplitude. The resonance order n represents the number of antinodes in the adhesive layer. It is noted that the curing of the adhesive increases the wave velocity c, which leads to the increase in the layer resonance frequencies f_n.

The schematic of the setup for measuring the resonance frequency is shown in Fig. 1. Rectangular-shaped A5052 aluminum alloy substrates of length 100 mm, width 20 mm, and thickness 2 mm were bonded with a two-

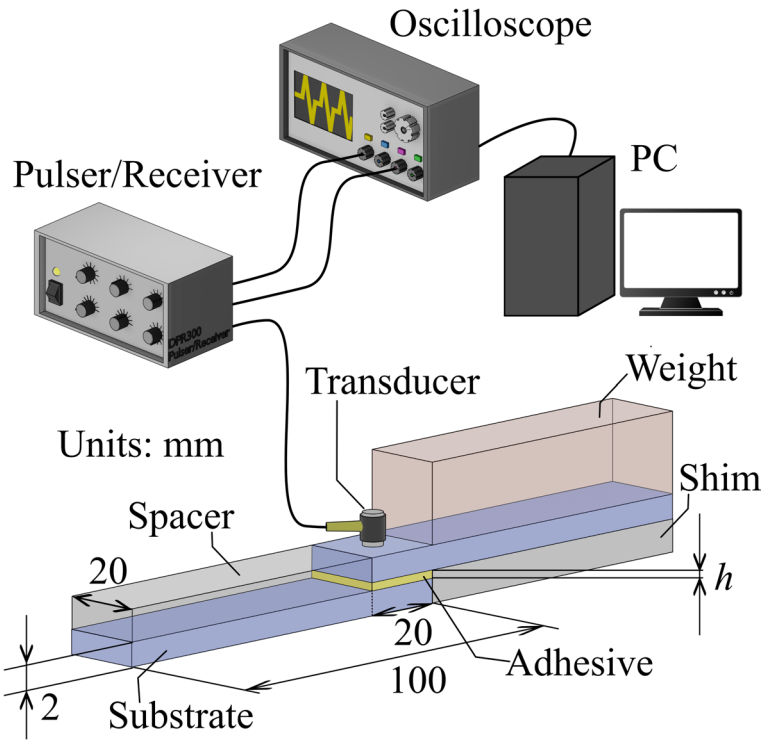

Fig. 1. Schematic of the setup for ultrasonic pulse-echo measurement.

component epoxy adhesive to produce a single lap joint. The bonding surfaces of the aluminum alloy substrates were prepared by sanding with #320 abrasive paper, rinsing with water, and drying them. To control the bond length and bond thickness, two plates with a length of 80 mm, a width of 20 mm, and a thickness of 2.2 mm were placed as shim and spacer. Namely, the bond length was 20 mm, and the bond thickness was set as approximately 0.2 mm. Two types of epoxy adhesives, namely, 2082 C (ThreeBond Co., Ltd.) and S6040 (Cemedine Co., Ltd.) were used to examine the effect of different adhesive types. The datasheets say that the pot lives of 2082 C and S6040 at a temperature of 25 ℃ are 70 min and 60 min, respectively, while the final curing time is the same, i.e., 24 h. It is noted that 2082 C contains rubber particles to enhance toughness.

After applying the adhesive on the substrate surfaces, the resonance frequency of the adhesive layer is measured by ultrasonic pulse-echo technique. As shown in Fig. 1, a piezoelectric transducer (V116-RM, Olympus) with a nominal frequency of 20 MHz and an element size of 3 mm was attached to the center of the overlap surface via an acoustic couplant (B2, Olympus). To prevent the deflection of the upper adherend, a weight was placed on its surface. A pulse voltage was supplied to the transducer with a pulse/receiver (DPR300, JPR Ultrasonics) to emit an incident longitudinal wave. The reflected waves were detected by the same transducer and pulser/receiver. The measured waveforms were recorded with an oscilloscope (MDO3014, Tektronix) after averaging 64 synchronized signals, and the data were transferred to a PC via LabVIEW.

The resonance frequencies of the adhesive layer can be identified by calculating reflection spectra[27]. The reflection waveform from the adhesive layer is extracted by an appropriate time gate and is analyzed by fast Fourier transform (FFT) to calculate the amplitude spectrum $A_R(f)$, where f denotes frequency. This procedure was also carried out for a single substrate. The reflected wave from the bottom surface of the substrate was measured to obtain the reference waveform, and the reference spectrum $I(f)$ was obtained by analyzing the reference waveform with FFT. The reflection spectrum for the adhesive layer was calculated by

$$|R| = \frac{A_{\mathrm{R}}(f)}{I(f)}, \tag{2}$$

which depends on frequency f.

To illustrate the measurement procedures and the curing behavior, the ultrasonic measurement was performed for the 2082 C adhesive every 3 min within its pot life. Figure 2(a) shows the reflection waveforms from the adhesive layer at the elapsed time of t_E = 0 min, 30 min, and 60 min, together with the reference waveform. The elapsed time t_E = 0 min corresponds to when the transducer was attached to the overlap surface. The measured waveforms were extracted by multiplying a Turkey window function in 0.6–1.4 μs with a taper ratio of 25% and were analyzed by FFT. Figure 2(b) shows the obtained amplitude spectra for the four waveforms in a frequency range of 4–8 MHz. The reflection spectra $|R|$ can be calculated by substituting the amplitude spectra to Eq. (2), as shown in Fig. 2(c).

Local minima appear in the reflection spectra of Fig. 2(c) due to the destructive interference of reflected wave components from the adhesive layer. Their frequencies correspond to the layer resonance frequencies, which are theoretically given by Eq. (1). The interval between the adjacent resonance frequencies implies that the local minimum frequencies located in 4.2–4.7 MHz and 6.5–7.0 MHz correspond to the 2nd-order and 3rd-order resonance frequencies, respectively. The resonance frequencies f_2 and f_3 are extracted as functions of the elapsed time t_E, as shown in Fig. 2(d). This figure shows that the resonance frequency f_2 increases from 4.21 MHz to 4.49 MHz as the curing proceeds in t_E < 60 min, while f_3 increases from 6.57 MHz to 6.99 MHz. This variation results from increasing wave velocity c due to the curing of the adhesive[27]. It is implied that the increase in the resonance frequencies from the initial state to the elapsed time t_E = 60 min is within 10%. It is noted that the resonance frequency f_3 initially decreases but immediately begins to increase. The reason for this decreasing behavior is not clear at present, but it might be related to the viscoelastic nature of the adhesive.

Ultrasonic resonance treatment

Figure 3(a) and (b) show the schematics of the ultrasonic resonance treatment proposed in this study. After setting substrates and applying an adhesive, the initial resonance frequency of the adhesive layer, f_I, is obtained by the ultrasonic measurement presented in the previous section, as shown in Fig. 3(a). Based on the measured resonance frequency, the ultrasonic resonance treatment is performed for the single lap joint, as shown in Fig. 3(b). A continuous wave signal is generated by a function generator (33500B, Keysight) and is amplified by an amplifier (WMA-300, Falco system) with a nominal magnification of 50x. The output peak-to-peak voltage from the function generator was set to be 3 V_{pp} based on the output voltage limitation of the amplifier. The amplified signal is supplied into an ultrasonic transducer V109-RM (Olympus) with a nominal frequency of 5 MHz and an element size of 12.7 mm to excite ultrasonic vibrations. It is noted that this transducer is different from the one for the resonance frequency measurement because of the excitation efficiency.

Two types of continuous wave signal inputs are examined in this study. First, the initial resonance frequency of the adhesive layer, f_I, was input into the function generator to send a sinusoidal signal, which was unchanged during the processing. The resonance frequency that was the closest to the nominal frequency of the transducer, i.e., 5 MHz, was chosen as the input frequency. This setting is quite simple, but as shown in Fig. 2(d), the resonance frequency of the adhesive layer tends to increase as the curing proceeds. In other words, the sinusoidal signal input at the frequency f_I excites the layer resonance only at the initial state.

A frequency sweep was applied in the second input signal to consider the resonance frequency shift by the curing. As shown in the previous section, the change in the layer resonance frequency is lower than 10% in the elapsed time t_E < 60 min. Thus, a continuous chirp signal with a time-varying frequency

$$f = f_{\mathrm{I}} + (t - mT)\, a f_{\mathrm{I}}, \quad mT \leq t < (m+1)\, T, \tag{3}$$

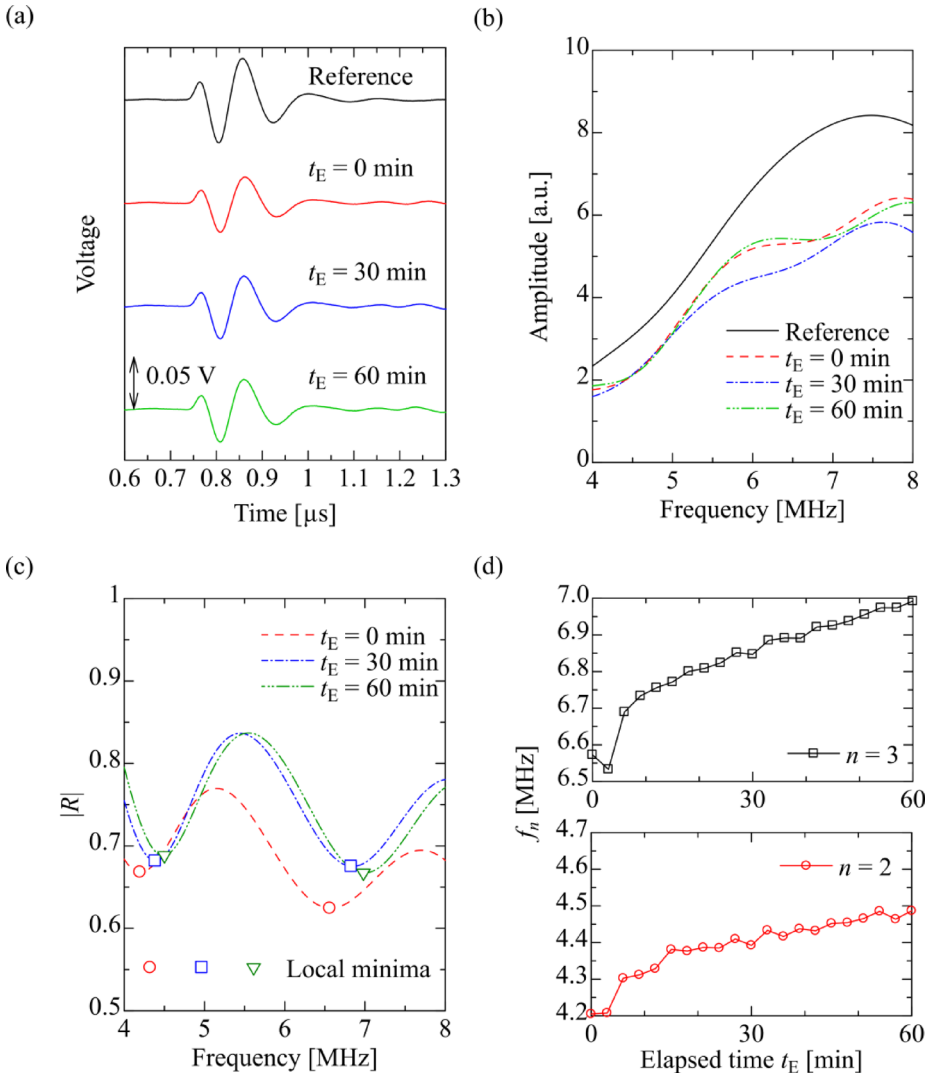

Fig. 2. Ultrasonic pulse-echo measurement for a curing adhesive layer within its pot life: variation of the (**a**) measured waveform, (**b**) amplitude spectrum, and (**c**) reflection spectrum with the elapsed time t_E. The changes in the 2nd-order and 3rd-order layer resonance frequencies f_2 and f_3 are shown in (**d**). The results correspond to the case of the 2082 C adhesive.

was sent by the function generator, where t is time, af_1 is a chirp ratio, $T = 1$ s is a chirp period, and $m = 0, 1, 2, \ldots$. Based on the measured frequency shifts in Fig. 2(d), the parameter a is set as $a = 0.1/T$. The frequency bandwidth of the chirp signal can cover shifting resonance frequency in longer durations than the sinusoidal signal. Namely, the effects of the ultrasonic layer resonance with chirp signals are expected to be more significant than with sinusoidal signals.

Ultrasonic processing time was set as 0 min, 30 min, and 60 min based on the pot lives of the two adhesives used in this study, approximately 60 min. Due to the limited number of instruments available, experiments for the inputs of single frequency and frequency sweep were conducted in different periods. This difference made the bonding conditions not completely identical. Thus, bonded specimens with and without the ultrasonic resonance treatment were produced simultaneously, and their bond strengths were compared for each input vibration type.

Tensile shear test and fracture surface observation

After passing the final curing time, i.e., 24 h, tabs made of the same aluminum alloy as the substrates, with a length of 37.5 mm and a width of 20 mm, were bonded on the substrates to conduct a tensile shear test. Loads were applied to the specimen by a universal testing machine (RTI-1310, A&D) at a crosshead displacement rate of 1 mm/min until the fracture. Load-displacement diagrams for several specimens are shown in Fig. 4. The measured loads tended to increase monotonically with increasing displacement until the fracture. The shear bonding strength was calculated as

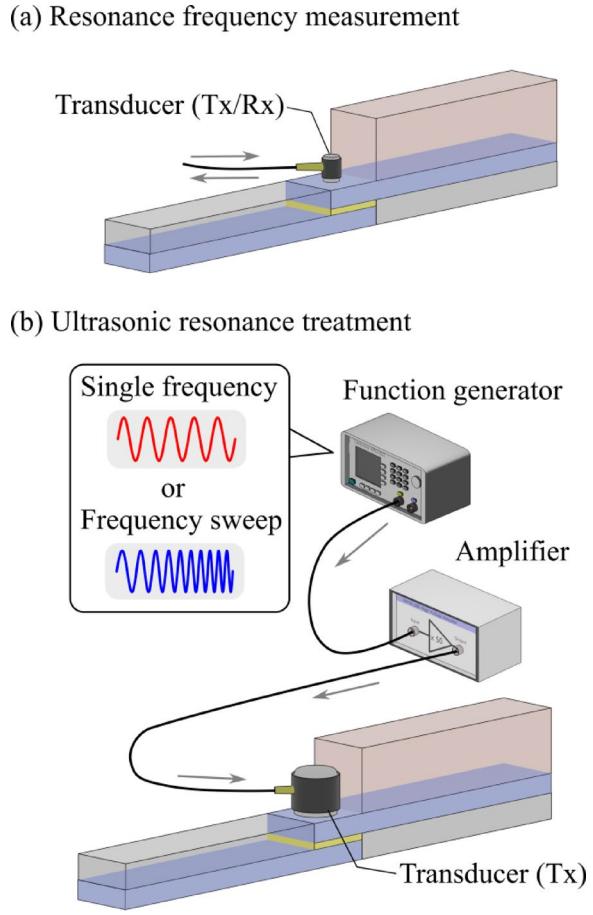

Fig. 3. Schematics of the procedures in the ultrasonic resonance treatment: (**a**) pulse-echo measurement for measuring the resonance frequency of an adhesive layer and (**b**) input of ultrasonic resonance vibrations.

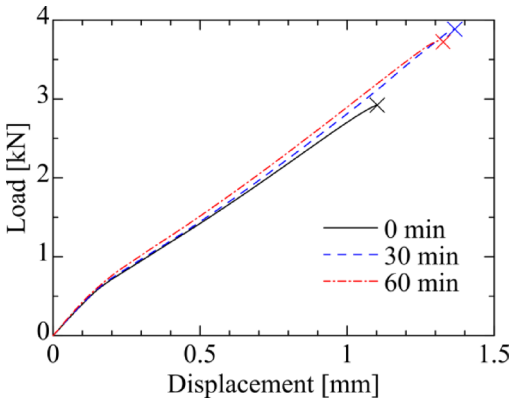

Fig. 4. Examples of load-displacement relations measured in tensile shear tests. The tested specimens correspond to the ones produced by the 2082 C adhesive and subjected to the ultrasonic resonance treatment with frequency sweep inputs for the processing times of 0 min, 30 min, and 60 min. The crossing symbols represent fracture points.

$$s_{\mathrm{b}} = \frac{P_{\max}}{A_{\mathrm{b}}}, \tag{4}$$

where $P_{\max}$ is the maximum load, and A_{b} is the bonding area of the specimen. It is noted that the effects of stress concentration at the edges of the joints are neglected in this configuration. This simple procedure was employed to examine the influences of the ultrasonic treatment on the curing of the adhesives. For each process condition,

the bonding strength was measured for at least three specimens. The average value and 95% confidence interval of the bonding strength were calculated and discussed. It is noted that a greater number of specimens would be required to evaluate the 95% confidence intervals more accurately.

After the tensile shear test, fracture surfaces were optically observed to evaluate the fracture configuration. A camera was mounted on a jig to control the distance and the angle to specimen surfaces. The horizontal and vertical directions of each specimen surface were carefully adjusted to those of the photograph. After acquiring images of 1108×1477 px, the parts corresponding to fracture surfaces were extracted as images of 206×206 px. An example of the observed results for a pair of fracture surfaces is shown in Fig. 5. Since cohesive fracture was not clearly confirmed, a quantity called fracture area ratio (FAR) was calculated to quantify the remaining adhesive area in this study. The images of the fracture surfaces were binarized with ImageJ (NIH, US) to differentiate the adherend surface and the remaining adhesive. In the binarized images shown in Fig. 5, the black and white areas correspond to the adherend and adhesive, respectively.

For each image, the number of pixels located in the white area, denoted as N_w, was counted and divided by that in the entire image, N. This provides the remaining adhesive ratio, i.e., $r = N_w/N$. A specimen after the test has two fracture surfaces, resulting in two different remaining adhesive ratios r_1 and r_2 ($0 \le r_1 < r_2 \le 1$). The fracture area ratio (FAR)

$$F_a = \frac{r_1 + (1 - r_2)}{2} \tag{5}$$

was calculated for each specimen. For example, when a bonded specimen exhibits complete interface fracture, the remaining adhesive ratios are $r_1 = 0$ and $r_2 = 1$. Thus, the FAR is obtained as $F_a = 0$. Namely, low FARs represent that the interface fracture is dominant.

Results

Ultrasonic treatment at an initially measured resonance frequency

The effects of the ultrasonic treatment at an initially measured layer resonance frequency f_I on the bond strength are presented in this section. Figure 6 summarizes the results of the shear bond strength and the fracture surface observation for three different ultrasonic processing times 0 min, 30 min, and 60 min. The 2082 C adhesive was used to produce the specimens. For each condition, four specimens were tested. The bar graphs and error bars show the averages and 95% confidence intervals of the bond strength, respectively. The measured bond strength without the resonance treatment was 7.37 ± 0.74 MPa while becoming 8.60 ± 0.12 MPa when the resonance treatment was processed for 30 min. Namely, this resonance treatment contributed to the increase in the average of the bond strength by 17% and the decrease in its variation by 84%. These results imply that the ultrasonic resonance treatment for the processing time of 30 min has slightly improved the bond strength. The FAR obtained by the fracture surface observation was approximately F_a = 25%, almost unchanged by the resonance treatment.

When the processing time of the resonance treatment increased to 60 min, the bond strength became 8.04 ± 2.19 MPa. The average value of the bond strength was still higher than the case without the treatment, but the variation almost tripled. It is ambiguous whether the bond strength has improved when the processing time was 60 min. Furthermore, the FAR obtained by the fracture surface observation did not show apparent changes by the resonance treatment.

Effect of frequency sweep

Since the input frequency for the ultrasonic treatment has been fixed at the initially measured resonance frequency in the previous section, the layer resonance would have occurred for a short duration after applying the adhesive because of the frequency shift by the curing process. In this section, the time-varying frequency expressed by Eq. (3) is input in the ultrasonic resonance treatment.

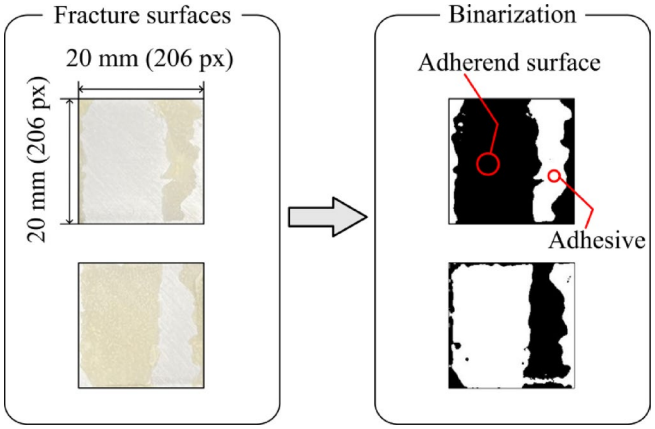

Fig. 5. Procedures for fracture surface analysis.

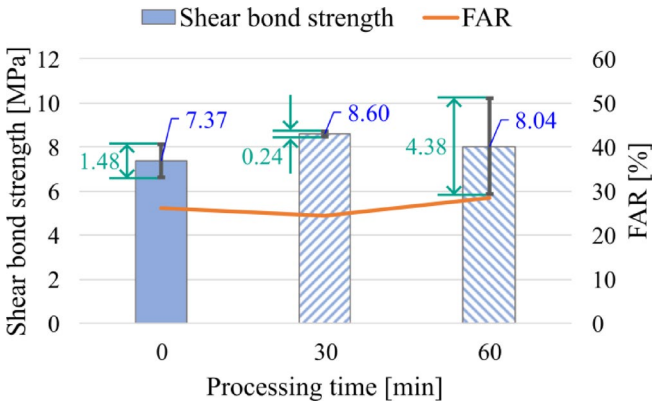

Fig. 6. Shear bond strengths of specimens bonded by the 2082 C adhesive and subjected to ultrasonic resonance treatment at an initially measured resonance frequency for different processing times. The FARs obtained by fracture surface observation are shown together.

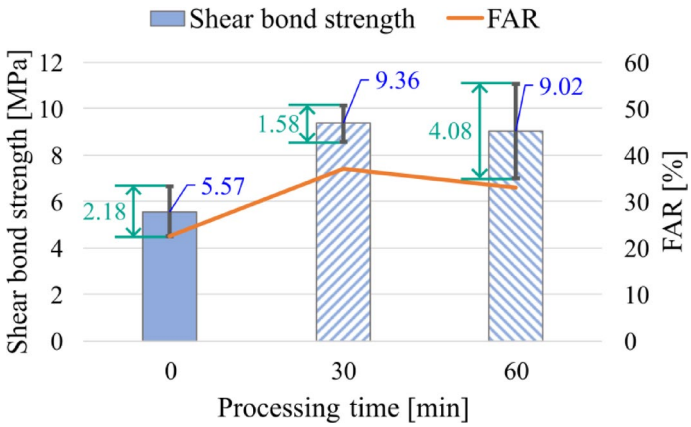

Fig. 7. Shear strengths of bonded specimens subjected to ultrasonic treatment with frequency sweeps for different processing times. The FARs obtained by fracture surface observation are shown together. The 2082 C adhesive was used to produce the specimens.

The results of the shear bond strength and the fracture surface observation are shown in Fig. 7 when the frequency sweep was applied for three different processing times 0 min, 30 min, and 60 min. Similarly to the previous section, the 2082 C adhesive was used to produce specimens. In the experiment, six specimens were tested for the processing time of 0 min, while the numbers of specimens for the processing times of both 30 min and 60 min were three. It can be seen in this figure that the resonance treatment has increased the average bond strength by 68% for the processing time of 30 min and by 62% for the processing time of 60 min. These increase ratios are relatively significant compared to when the initially measured resonance frequency is input in the ultrasonic treatment, as shown in Fig. 6. Furthermore, analogously to the results in the previous section, the 95% confidence interval decreased by the resonance treatment for 30 min, while increasing when the processing time was 60 min. Although the lower end of the 95% confidence interval for the processing time of 60 min was closer to the upper end for 0 min than the lower end for 30 min, the proposed resonance treatment tends to improve the bond strength for both processing times of 30 min and 60 min. A similar trend can be seen in the results of the fracture surface observation. Compared to the case without the resonance treatment, the FAR increased by 14% and 10% for the processing times of 30 min and 60 min, respectively.

For the bonded specimens used to obtain the data in Fig. 7, the bond thicknesses were measured with a micrometer gauge before the fracture tests, as shown in Fig. 8. The bond thickness for each processing time was approximately 0.20 mm, which is close to the nominal thickness based on the thickness gap between the substrate and shim. Figure 8 shows that apparent differences are not confirmed in the bond thicknesses between the processing times of 0 min and 30 min, while the average bond thickness for the processing time of 60 min is lower than the other two cases. Previous papers on ultrasonic treatment at low frequencies[16,17] reported that input vibrations can reduce bond thickness, implying an enhancement in the fluidity of adhesives. However, as seen in Fig. 8, this effect does not appear to be clearly confirmed in the resonance treatment of the present study.

In the above experiments, the input frequency f_I for the frequency sweep was chosen as the initial resonance frequency closest to 5 MHz, which is the nominal frequency of the transducer. To examine the effect of different

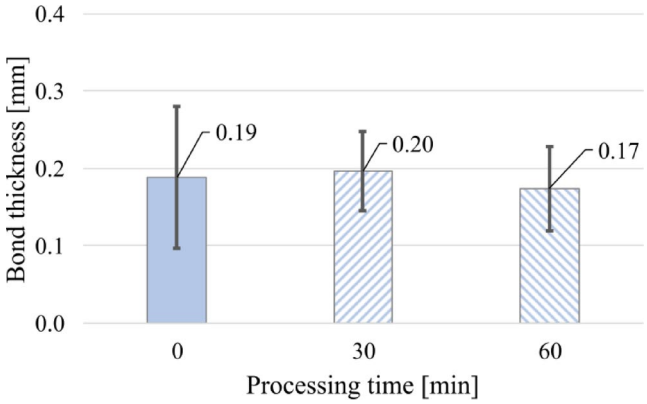

Fig. 8. Bond thicknesses of specimens subjected to ultrasonic treatment with frequency sweeps for different processing times. The data shown in Fig. 7 were based on these bonded specimens.

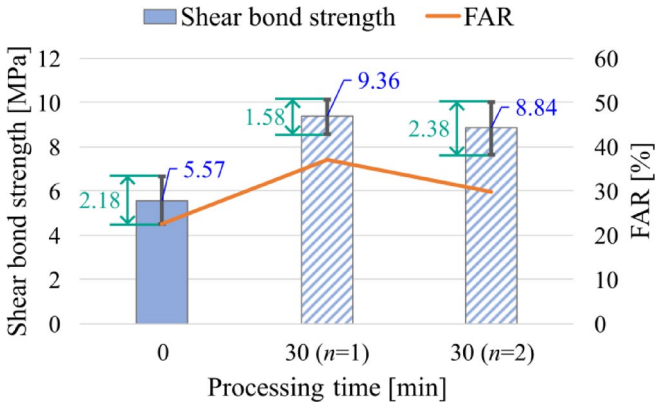

Fig. 9. Effect of resonance mode order n on the shear strengths of bonded specimens subjected to the ultrasonic treatment with frequency sweeps. The FARs obtained by fracture surface observation are shown together. The 2082 C adhesive was used to produce the specimens.

resonance modes, ultrasonic treatments were performed for two different resonance orders $n=1$ and $n=2$. At the initial state, the measured 1st-order and 2nd-order resonance frequencies f_1 and f_2 were located in frequency ranges of 3.60–4.80 MHz and 7.10–9.12 MHz, respectively. This suggests that the transducer was able to excite vibrations more effectively at the 1st-order resonance frequency f_1 than at the 2nd-order resonance frequency f_2.

Figure 9 shows the results of the shear bond strength and the fracture surface observation for the resonance orders $n=1$ and $n=2$. The 2082 C adhesive was used to produce the specimens. The data for the processing times of 0 min and 30 min at $n=1$ are identical to those in Fig. 7. The number of specimens for the processing time of 30 min at $n=2$ was the same as that for $n=1$, three. The 2nd-order resonance treatment for the processing time of 30 min increased the average bond strength by 59% compared to the case for the processing time of 0 min. This result is similar to the resonance treatment at the order $n=1$, but a decrease in the 95% confidence interval was not confirmed at $n=2$. The relation between the nominal frequency of the transducer and the range of the resonance frequency might have affected the tendency. Nevertheless, the ultrasonic treatments for both resonance orders improved the average of the bond strength. This feature is consistent with the increase in the FAR shown in Fig. 9.

Effects of vibration amplitude and adhesive type

The previous section has shown that the frequency sweep considering the resonance frequency shift by the curing process of the adhesive can enhance the effects of the ultrasonic treatment. This section explores two other factors that can affect the bonding strength: vibration amplitude and adhesive type.

The effect of the vibration amplitude imposed on the joint was investigated by eliminating the amplifier shown in Fig. 3. In other words, the output voltage from the function generator was supplied directly to the transducer without the amplifier. The peak-to-peak amplitude of the output signal from the function generator was set to be 10 V_{pp}, which is lower than the 10% of the output voltage from the amplifier. The frequency sweep was applied to the input signals, similarly to the previous section.

Figure 10 shows the results of the fracture tests when weak vibrations were excited for three processing times. Similarly to the previous sections, the 2082 C adhesive was used to produce the specimens. For each

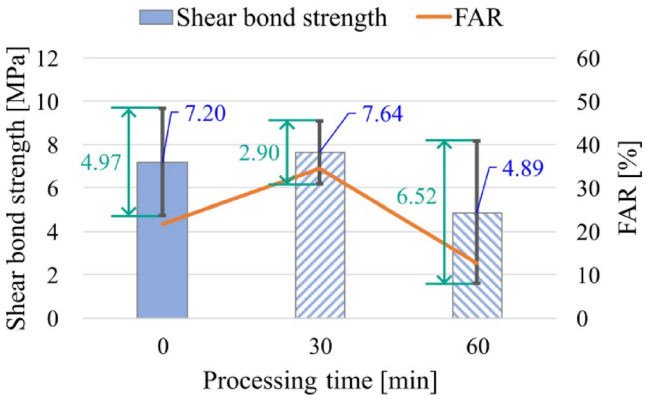

Fig. 10. Shear strengths of bonded specimens subjected to ultrasonic resonance treatment with frequency sweeps without the amplifier for different processing times. The FARs obtained by fracture surface observation are shown together. The 2082 C adhesive was used to produce the specimens.

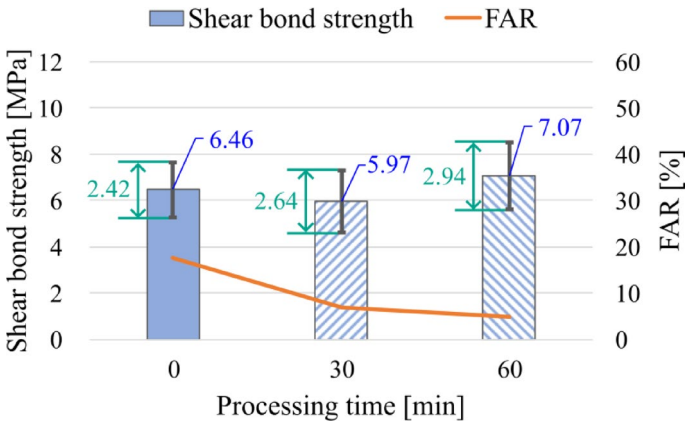

Fig. 11. Effects of ultrasonic treatment with frequency sweeps for the S6040 adhesive on bond strength. The FARs obtained by fracture surface observation are shown together.

condition, three specimens were tested. The average shear bond strength and the FAR for the processing time of 30 min was higher than those without the resonance treatment, respectively, but its effect was unclear because of variations. Similarly, the variation of the bond strength for the processing time of 60 min makes the effect of the resonance treatment more ambiguous. Although a greater number of specimens might be necessary to evaluate the 95% confidence intervals more precisely, the increase in the variation for the processing time of 60 min seems consistent with the result that the FAR of this condition was low compared to that without the resonance treatment. Both features imply that interface fracture occurred more frequently for the processing time of 60 min. The above results suggest that the ultrasonic resonance treatment with the low input voltage does not apparently improve adhesion between substrate and adhesive. This implies that the input voltage has a threshold to enhance bond strength effectively, which is not further explored in the present study.

In the above experiments, ultrasonic treatments have been examined for the 2082 C adhesive, but their effect can differ if the adhesive has different properties. To explore how the adhesive type affects the results, the S6040 adhesive was employed for the proposed treatment. This adhesive does not contain rubber particles, which means that its toughness is lower than that of the 2082 C adhesive. The treatment procedures are the same as described in the previous sections. Namely, a chirp signal based on the initially measured resonance frequency f_I was generated by the function generator and then supplied to the transducer via the amplifier.

Figure 11 shows the shear bond strength and the FAR when the resonance treatment was applied to the S6040 adhesive for the processing times 0 min, 30 min, and 60 min. In the experiment, six specimens were tested for the processing time of 0 min, while the numbers of specimens for the processing times of both 30 min and 60 min were three. It is found that the average shear bond strength has slightly decreased and increased for the processing times of 30 min and 60 min, respectively. However, their variations show that the change in the bond strength was insignificant compared to the results for the 2082 C adhesive. On the other hand, the FAR tended to decrease with increasing processing time. These features show that the ultrasonic treatment did not apparently improve adhesion in the case of the S6040 adhesive.

Discussion

The previous sections have shown that the proposed ultrasonic resonance treatment improved bond strength when frequency sweeps were adopted for the 2082 C adhesive. As shown in Fig. 7, this treatment has also enhanced the FAR of the fracture surfaces, which implies that fracture occurred more frequently in bond layers. These features suggest that wettability between substrate and adhesive has been improved by the resonance treatment. Additionally, a previous paper[15] reported that ultrasonic treatment at low frequencies acts to eliminate contamination on adherend surfaces. A similar effect might be expected in the proposed resonance treatment of the present study.

The comparison between Figs. 6 and 7 shows that frequency sweeps facilitate the effectiveness of the resonance treatment. This trend appears probably because the resonance frequencies of the adhesive layer increase as the curing proceeds, as shown in Fig. 2(d). If the input frequency in the resonance treatment is fixed at the initial resonance frequency, the effective duration for which the layer resonance occurs becomes short compared to the entire processing time. In other words, a frequency sweep is expected to allow the layer resonance to last longer in the processing period. This effect leads to the improvement of bond strength, which seems consistent with the results for the FAR.

On the other hand, longer processing times do not necessarily lead to higher bond strength. As shown in Fig. 7, the average bond strength for the processing time of 60 min was slightly lower than the one for 30 min, and the variation in bond strength increased. This deterioration may be associated with the pot life of the 2082 C adhesive, i.e., 70 min. The liquidity of adhesives plays an important role in improving the wettability between the adhesive and adherend. Curing reactions would accelerate around the pot life of the adhesive, resulting in its transition from a liquid-like to a solid-like state. If the resonance treatment continues until the pot life, it could interfere with the bonding formation between the substrate and adhesive. This issue was also addressed in previous papers on ultrasonic-assisted adhesive bonding[17]. In the present study, the shims may have constrained the curing adhesive, resulting in weakening effects due to the long ultrasonic processing time. Stopping the resonance treatment just before the polymerization initiates might maximize the effect of the proposed method. This fact implies the necessity to pay attention to the input vibration amplitude. Excessively strong vibrations could disturb the bonding between substrate and adhesive. Thus, determining the optimal processing condition would be necessary based on the nature of the adhesive. To this purpose, a broader range of processing conditions should be considered in future work.

Interestingly, the proposed ultrasonic resonance treatment has improved bond strength for the 2082 C adhesive but had ambiguous effects on the S6040, as shown in Figs. 7 and 11. A notable difference between the two adhesives is that the 2082 C adhesive contains rubber particles to enhance its toughness. Previous studies on ultrasonic-assisted adhesive bonding[17] showed that whether the adhesive is brittle or ductile affects the effectiveness of the ultrasonic treatment. They demonstrated that in the case of brittle adhesives, microbubbles generated in uncured adhesives by ultrasonic vibrations serve as defects that lower the bond strength. On the other hand, this effect was shown to be not conspicuous if the adhesive is ductile. Similar trends probably appear in the ultrasonic resonance treatment proposed in the present study. It can be expected that rubber particles located in the vicinity of adhesive interfaces prevent crack initiation along the interfaces, facilitating fracture inside the adhesive layer. This change may bring an improvement in bond strength.

This paper has demonstrated that the proposed resonance treatment can contribute to increasing bond strength, but processing conditions and adhesive types affect its effectiveness. Specifically, improvements in bond strength have not been confirmed in the case of the adhesive S6040, which might be attributed to a limited set of processing conditions tested. In future work, it will be essential to reveal specific physical mechanisms involved in the proposed treatment, which may help identify optimal processing conditions. Furthermore, integrating an ultrasonic curing monitoring technique[27] with the proposed resonance treatment could provide information about the ideal processing duration.

Conclusions

In the present study, a layer resonance phenomenon induced by high-frequency ultrasonic vibrations has been applied to a preprocessing treatment to improve adhesion between metal substrate and adhesive. The proposed resonance treatment consists of two steps, i.e., resonance frequency measurement by ultrasonic pulse-echo technique and ultrasonic vibration input. The effects of the proposed method on shear bond strength have been examined for single lap joints. For an adhesive containing rubber particles, the bond strength has improved by the resonance treatment for the processing time of 30 min, which is shorter than the pot life of the adhesive, 70 min. In particular, the resonance treatment with frequency sweeps considering the resonance frequency shift by the curing process has enhanced bond strength. However, its effectiveness has slightly declined if the processing time is close to the pot life, i.e., 60 min. It has been shown that the increase in the bond strength by the proposed treatment is associated with the fracture area ratio (FAR) representing fracture inside adhesive layers. On the other hand, the resonance treatment for an adhesive without rubber particles has not improved bond strength. The proposed treatment has the potential to enhance adhesion between substrate and adhesive, but the treatment conditions should be determined carefully depending on the nature of the adhesive.

Data availability

Data will be made available from the corresponding author upon reasonable request.

Received: 22 April 2025; Accepted: 10 September 2025
Published online: 14 October 2025

References

1. Harris, A. F. & Beevers, A. The effects of grit-blasting on surface properties for adhesion. *Int. J. Adhes. Adhes.* **19**, 445–452 (1999).
2. Rudawska, A., Danczak, I., Müller, M. & Valasek, P. The effect of sandblasting on surface properties for adhesion. *Int. J. Adhes. Adhes.* **70**, 176–190 (2016).
3. Park, Y. J., Shin, K. H. & Song, H. J. Effects of anodizing conditions on bond strength of anodically oxidized film to titanium substrate. *Appl. Surf. Sci.* **253**, 6013–6018 (2007).
4. Abrahami, S. T., Hauffman, T., de Kok, J. M. M., Mol, J. M. C. & Terryn, H. Effect of anodic aluminum oxide chemistry on adhesive bonding of epoxy. *J. Phys. Chem. C Nanomater Interfaces.* **120**, 19670–19677 (2016).
5. Rotel, M., Zahavi, J., Tamir, S., Buchman, A. & Dodiuk, H. Pre-bonding technology based on excimer laser surface treatment. *Appl. Surf. Sci.* **154–155**, 610–616 (2000).
6. Fischer, F. et al. Laser surface pre-treatment of CFRP for adhesive bonding in consideration of the absorption behaviour. *J. Adhes.* **88**, 350–363 (2012).
7. Kurtovic, A., Brandl, E., Mertens, T. & Maier, H. J. Laser induced surface nano-structuring of Ti–6Al–4V for adhesive bonding. *Int. J. Adhes. Adhes.* **45**, 112–117 (2013).
8. Palmieri, F. L., Belcher, M. A., Wohl, C. J., Blohowiak, K. Y. & Connell, J. W. Laser ablation surface Preparation for adhesive bonding of carbon fiber reinforced epoxy composites. *Int. J. Adhes. Adhes.* **68**, 95–101 (2016).
9. Wu, Y. et al. Effect of laser ablation surface treatment on performance of adhesive-bonded aluminum alloys. *Surf. Coat. Technol.* **304**, 340–347 (2016).
10. Wang, H., Hao, X., Zhou, H., Li, D. & Hua, L. Study on ultrasonic vibration-assisted adhesive bonding of CFRP joints. *J. Adhes. Sci. Technol.* **30**, 1842–1857 (2016).
11. Wang, H., Hao, X., Yan, K., Zhou, H. & Hua, L. Ultrasonic vibration-strengthened adhesive bonding of CFRP-to-aluminum joints. *J. Mater. Process. Technol.* **257**, 213–226 (2018).
12. Yan, L., Chen, W., Li, H. & Zhang, Q. Mechanism of ultrasonic vibration effects on adhesively bonded ceramic matrix composites joints. *Ceram. Int.* **47**, 33214–33222 (2021).
13. Wang, H., Kang, G., Chen, Y., Liu, Z. & Hua, L. Reducing interface defects and porosity of adhesive bonded aluminum alloy joints via ultrasonic vibration. Polymers (Basel) **15**, 2098 (2023).
14. Zhou, Z. & Chen, C. Research advances in the ultrasonic-assisting adhesive bonding. *J. Manuf. Process.* **110**, 134–160 (2024).
15. Holtmannspötter, J., Czarnecki, J. & Gudladt, H. J. The use of power ultrasound energy to support interface formation for structural adhesive bonding. *Int. J. Adhes. Adhes.* **30**, 130–138 (2010).
16. Yuan, W. et al. Enhancing mechanical properties of adhesive laminates joints using ultrasonic vibration-assisted preprocessing. *Compos. Struct.* **227**, 111325 (2019).
17. Yang, G. & Yuan, W. The influence of ultrasonic vibration-assisted processing on mode-I fracture toughness of CFRP-bonded joints. *Int. J. Adhes. Adhes.* **104**, 102742 (2021).
18. Wang, H. et al. Study on ultrasonic vibration-assisted adhesive bonding of CFRP laminates with laser ablation-treated surfaces. *Compos. Struct.* **268**, 113983 (2021).
19. Ma, Z. et al. Controlled tough bioadhesion mediated by ultrasound. *Science* **377**, 751–755 (2022).
20. Pialucha, T. & Cawley, P. The detection of thin embedded layers using normal incidence ultrasound. *Ultrasonics* **32**, 431–440 (1994).
21. Dixon, S., Lanyon, B. & Rowlands, G. Ultrasonic resonance in thin two-layer dynamic systems. *J. Phys. D Appl. Phys.* **39**, 506–514 (2006).
22. Mori, N., Matsuda, N. & Kusaka, T. Effect of interfacial adhesion on the ultrasonic interaction with adhesive joints: A theoretical study using spring-type interfaces. *J. Acoust. Soc. Am.* **145**, 3541 (2019).
23. Mori, N., Iwata, Y., Hayashi, T. & Matsuda, N. Viscoelastic wave propagation and resonance in a metal–plastic bonded laminate. *Mech. Adv. Mater. Struct.* **30**, 3803–3816 (2023).
24. Mori, N. & Hayashi, T. Ultrasonic interference and critical Attenuation in metal-plastic bilayer laminates. *J. Sound Vib.* **547**, 117531 (2023).
25. Mori, N., Okabe, T. & Hayashi, T. Polymer coating characterization based on ultrasonic interference and critical Attenuation. *Struct. Health Monit. Press.* https://doi.org/10.1177/14759217251333460
26. Allin, J. M., Cawley, P. & Lowe, M. J. S. Adhesive disbond detection of automotive components using first mode ultrasonic resonance. *NDT&E Int.* **36**, 503–514 (2003).
27. Mori, N., Hakkaku, T. & Hayashi, T. Curing monitoring of adhesive layers between metal adherends by ultrasonic resonance technique. *Meas. Sci. Technol.* **36**, 015605 (2025).

Acknowledgements

This study has been supported by Grants-in-Aid for Scientific Research (KAKENHI) Grant No. 23K03590 from Japan Society for the Promotion of Science (JSPS).

Author contributions

Toru Hakkaku: Methodology (support), Validation (lead), Formal analysis (lead), Investigation (lead), Data curation (lead), Visualization, Writing – original draft (equal), Writing – review & editing (equal).Naoki Mori: Conceptualization, Methodology (lead), Software (lead), Validation (support), Formal analysis (support), Investigation (support), Data curation (support), Writing – original draft (equal), Writing – review & editing (equal), Supervision (lead).Takahiro Hayashi: Methodology (support), Software (support), Data curation (support), Writing – review & editing (equal), Supervision (support).

Declarations

Competing interests

The authors declare no competing interests.

Additional information

Correspondence and requests for materials should be addressed to N.M.

Reprints and permissions information is available at www.nature.com/reprints.

Publisher's note Springer Nature remains neutral with regard to jurisdictional claims in published maps and institutional affiliations.